RadioGraphics

Radiologic Manifestations of Sarcoidosis in Various Organs[1]

Takashi Koyama, MD • Hiroyuki Ueda, MD • Kaori Togashi, MD
Shigeaki Umeoka, MD • Masako Kataoka, MD • Sonoko Nagai, MD

CME FEATURE

See accompanying test at http://www.rsna.org/education/rg_cme.html

LEARNING OBJECTIVES FOR TEST 3

After reading this article and taking the test, the reader will be able to:

- Recognize both typical and atypical imaging features of sarcoidosis in various anatomic locations.
- Describe clinical manifestations that play an important role in diagnosing sarcoidosis.
- Discuss various clinical settings and syndromes that are related to sarcoidosis.

Sarcoidosis is a systemic disorder of unknown cause with a wide variety of clinical and radiologic manifestations. The diagnosis is usually made on the basis of these manifestations supported by histologic findings. Systemic manifestations (eg, Löfgren syndrome, Heerfordt syndrome) are commonly seen at clinical examination. Bilateral hilar lymphadenopathy is the most common radiologic finding—frequently with associated pulmonary infiltrates—and typically has a characteristic perivascular distribution at high-resolution chest computed tomography. Radiologic findings in the short tubular bones of the hands and feet and magnetic resonance imaging findings of nodular involvement of muscle are often sufficient to raise suspicion for sarcoidosis. In the liver, spleen, kidneys, and scrotum, coalescing granulomas form nodules whose imaging features may occasionally be nonspecific, although familiarity with the relevant clinical settings will be helpful in recognizing the presence of sarcoidosis. Radiologic recognition of cardiac and central nervous system involvement is also important because patients may be only mildly symptomatic. The clinical course and prognosis of sarcoidosis are highly variable, often correlating with the mode of onset. Familiarity with the clinical and radiologic features of sarcoidosis in various anatomic locations plays a crucial role in diagnosis and management.

Abbreviations: ACE = angiotensin-converting enzyme, CNS = central nervous system, FLAIR = fluid-attenuation inversion recovery

Index terms: Abdomen, diseases, 70.22, 76.22, 77.22, 81.22, 847.22 • Head and neck, 20.22 • Nervous system, diseases, 10.22, 30.22 • Sarcoidosis, **.22 • Thorax, diseases, 51.22, 60.22, 679.22

RadioGraphics 2004; 24:87–104 • **Published online** 10.1148/rg.241035076

[1]From the Department of Radiology, Kyoto University Hospital, 54 Kawahara-cho, Shogoin, Sakyo-ku, Kyoto 606-8507, Japan (T.K., H.U.); and the Departments of Diagnostic and Interventional Imageology (K.T.), Nuclear Medicine and Diagnostic Imaging (S.U., M.K.), and Respiratory Medicine (S.N.), Graduate School of Medicine, Kyoto University of Medicine, Kyoto, Japan. Recipient of a Certificate of Merit award for an education exhibit at the 2002 RSNA scientific assembly. Received March 21, 2003; revision requested April 23 and received August 28; accepted August 28. All authors have no financial relationships to disclose. **Address correspondence to** T.K. (e-mail: *montpeti@kuhp.kyoto-u.ac.jp*).

[2]**. multiple body systems

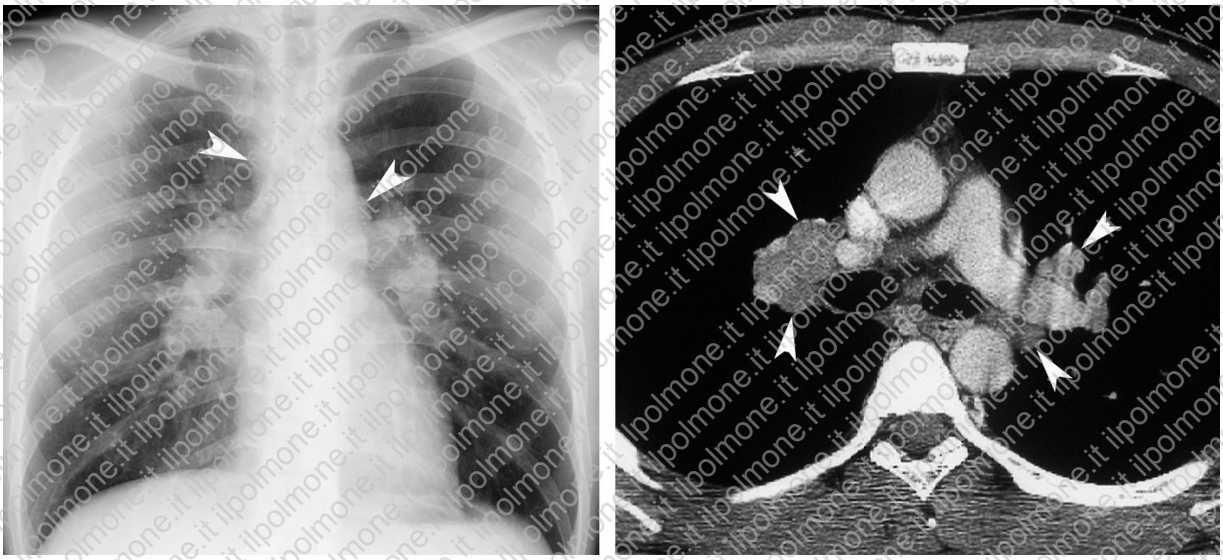

a. b.

Figure 1. Hilar adenopathy in a 27-year-old man with Heerfordt syndrome. **(a)** Chest radiograph demonstrates typical bilateral hilar adenopathy. Adenopathy in the right paratracheal and left aortic-pulmonary window nodes (arrowheads) is also identified. **(b)** Contrast material–enhanced computed tomographic (CT) scan clearly depicts the bilateral hilar adenopathy (arrowheads).

Introduction

Sarcoidosis is a systemic disorder of unknown cause that is characterized by noncaseating granulomas with proliferation of epithelioid cells. Sarcoidosis commonly affects young and middle-aged patients, with a slightly higher prevalence in women (1). The disease has distinct geographic and racial predilections, with African-Americans, Swedes, and Danes appearing to be most commonly affected (1). Although some other areas, including Japan, are also known to have a high prevalence of sarcoidosis, recognition of the disease may be limited in part by a mass screening system in these countries. Clinical signs and symptoms are nonspecific and include fatigue, weight loss, general malaise, and, less commonly, fever. About one-half of patients remain asymptomatic. Bilateral hilar lymphadenopathy is the most common radiologic finding. Adenopathy in the right paratracheal nodes, left aortic-pulmonary window, and subcarinal nodes can also be seen, often with associated pulmonary infiltrates. However, extrathoracic involvement can be an initial manifestation in one-half of symptomatic patients. Although skin and ocular lesions are common, the liver, spleen, lymph nodes, parotid glands, central nervous system (CNS), genitourinary system, muscles, and bones may also be involved.

In this article, we review sarcoidosis in terms of diagnosis, clinical course and treatment, and clinical and radiologic manifestations in a variety of organs. We discuss and illustrate thoracic, CNS, head and neck, upper abdominal, genitourinary, musculoskeletal, and cutaneous involvement by sarcoidosis, knowledge of which can play a crucial role in diagnosis and management.

Diagnosis

The diagnosis of sarcoidosis is commonly established on the basis of clinical and radiologic findings supported by histologic findings. Lung biopsy specimens can be obtained with transbronchial biopsy or from extrapulmonary sites such as the cervical lymph nodes and liver. Pathologic findings in sarcoidosis consist of noncaseating granulomas with epithelioid cells and large, multinucleated giant cells. However, granulomas from other inflammatory processes such as tuberculosis, histoplasmosis and fungal infections, and tumor-related sarcoid reaction need to be excluded. In the past, the Kveim test was used for diagnosis; however, this test is no longer considered specific for sarcoidosis. Laboratory data show that the angiotensin-converting enzyme (ACE) level is commonly elevated and may correlate with disease activity. The CD4:CD8 ratio in the blood serum is commonly decreased. These abnormalities are helpful in making the diagnosis of sarcoidosis, although they may also be seen in other granulomatous diseases. Hypercalcemia is occasionally seen due to increased intestinal

Figure 2. Mediastinal adenopathy in a 26-year-old man who presented with severe back pain. Chest radiograph demonstrates markedly enlarged right paratracheal nodes. Left aortic-pulmonary window nodes with associated minimal hilar involvement are also seen.

absorption of calcium, which results from activation of vitamin D by macrophages in sarcoid granulomas.

Clinical Course and Treatment

The clinical expression, natural history, and prognosis of sarcoidosis are highly variable, with a tendency to wax and wane. The course and prognosis may correlate with the mode of onset and the extent of disease (1). Acute onset with erythema nodosum or asymptomatic bilateral hilar lymphadenopathy usually portends a self-limiting course with spontaneous resolution, whereas insidious onset, especially with lung involvement or multiple extrapulmonary lesions, may be followed by progressive fibrosis of the lung and other organs.

Sarcoidosis is the direct cause of death in 5% of patients (1). Attributable causes of death differ significantly depending on geographic location. In Japan, nearly 80% of patients die from cardiac involvement, whereas most patients in the United States die from pulmonary complications (2,3).

Corticosteroids are effectively used for treatment. Although some patients respond rapidly, others may require long-term therapy. In cases of aggressive disease or frequent recurrence, immunosuppressive drugs such as methotrexate and cyclophosphamide may be required.

Thoracic Involvement

Pulmonary involvement is reported in up to 90% of patients with sarcoidosis and generally manifests as asymptomatic mediastinal adenopathy

Figure 3. Mediastinal adenopathy in a 60-year-old man. Unenhanced chest CT scan demonstrates calcification in the affected hilar nodes, a finding that suggests a long clinical course. Note the simultaneous presence of huge subcarinal lymph nodes (arrowheads), an unusual finding in other granulomatous diseases such as tuberculosis.

(1). Hilar adenopathy is easily recognized on chest radiographs (Fig 1). However, CT is superior for demonstrating subtle mediastinal lymphadenopathy and associated parenchymal involvement. Because the prevalence of pulmonary involvement in patients with sarcoidosis is extremely high, CT findings play a crucial role in the diagnosis and staging of this disease. There are five radiologic stages of intrathoracic changes (1): Stage 0, normal chest radiograph; stage 1, lymphadenopathy only; stage 2, lymphadenopathy with parenchymal infiltration; stage 3, parenchymal disease only; and stage 4, pulmonary fibrosis. One-half of patients present with stage 1 disease.

Mediastinal Lymph Nodes

Intrathoracic lymphadenopathy is the most commonly encountered radiologic finding in sarcoidosis (85% of cases) and typically manifests as bilateral hilar adenopathy with right paratracheal adenopathy (4). Although left paratracheal and aortic-pulmonary window nodes are also commonly enlarged, these nodes are less easily identified on posteroanterior chest radiographs. This mediastinal adenopathy is successfully demonstrated at contrast-enhanced CT. Mediastinal adenopathy without hilar involvement is rare and is more frequently seen in older patients (Fig 2) (5). Occasionally, calcification occurs in affected nodes (Fig 3) (6). Calcification can be amorphous, punctate, or eggshell-like (4,6); it is closely related to the duration of the disease and suggests a chronic condition.

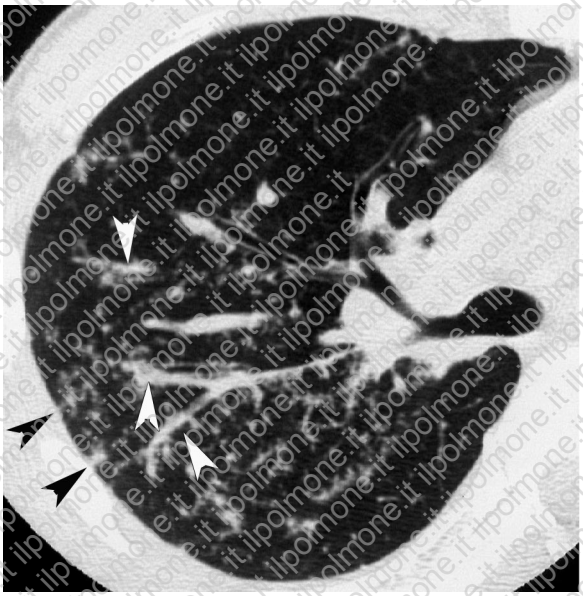

Figure 4. Pulmonary sarcoidosis in a 37-year-old man. High-resolution chest CT scan demonstrates small nodules with a perivascular distribution and irregular thickening of bronchovascular bundles (white arrowheads) and interlobular septa (black arrowheads). These findings reflect the pathologic distribution of sarcoid granulomas along the lymphatic vessels within interstitial tissue.

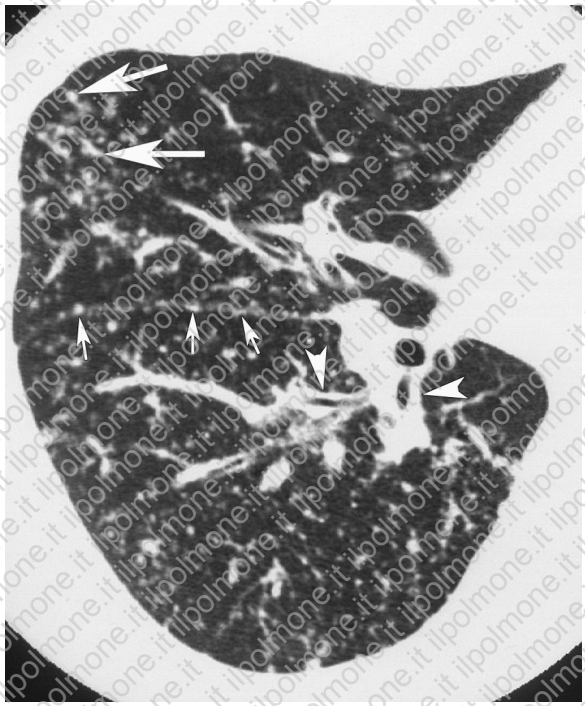

Figure 5. Pulmonary sarcoidosis in a 24-year-old man. High-resolution chest CT scan demonstrates multiple miliary nodules and diffuse thickening of the bronchial wall (arrowheads). Note the simultaneous presence of small nodules with a perivascular distribution (large arrows) and along the interlobular pleura (small arrows).

Lungs

Lung involvement is seen in approximately 20% of patients. Dyspnea and dry cough are common manifestations, whereas hemoptysis is rare. Lung involvement in sarcoidosis has a strong predilection for the upper lung.

At histologic analysis, sarcoid granulomas in the lung are typically distributed along the lymphatic vessels, which run within the interstitial tissues of bronchovascular bundles and the subpleural and perilobular spaces (7). High-resolution CT can accurately depict this characteristic distribution and typically demonstrates multiple small nodules in a perivascular distribution, along with irregular thickening of bronchovascular bundles and interlobular septa (Fig 4) (4,8,9). The pattern of distribution, upper lung predominance, and coexistence of mediastinal lymphadenopathy strongly indicate the presence of sarcoidosis, helping distinguish it from other nodular lesions such as eosinophilic granuloma, miliary tuberculosis, or metastasis. The CT appearance may occasionally mimic that of lymphangitis carcinomatosa or lymphoproliferative disorders; however, these diseases do not demonstrate an upper lobe predominance and are usually rapidly progressive with a worse clinical course. Other findings at high-resolution CT include multiple miliary nodules (Fig 5), bronchial wall thickening, and ground-glass attenuation (Fig 6); the latter may reflect the presence of microscopic interstitial granulomas. The simultaneous presence of small nodules with a perivascular or subpleural distribution can raise suspicion for sarcoidosis. Occasionally, coalescing granulomas can form multiple masslike nodules. Unlike metastatic disease, these nodules have irregular margins and may contain an air bronchogram (Fig 7).

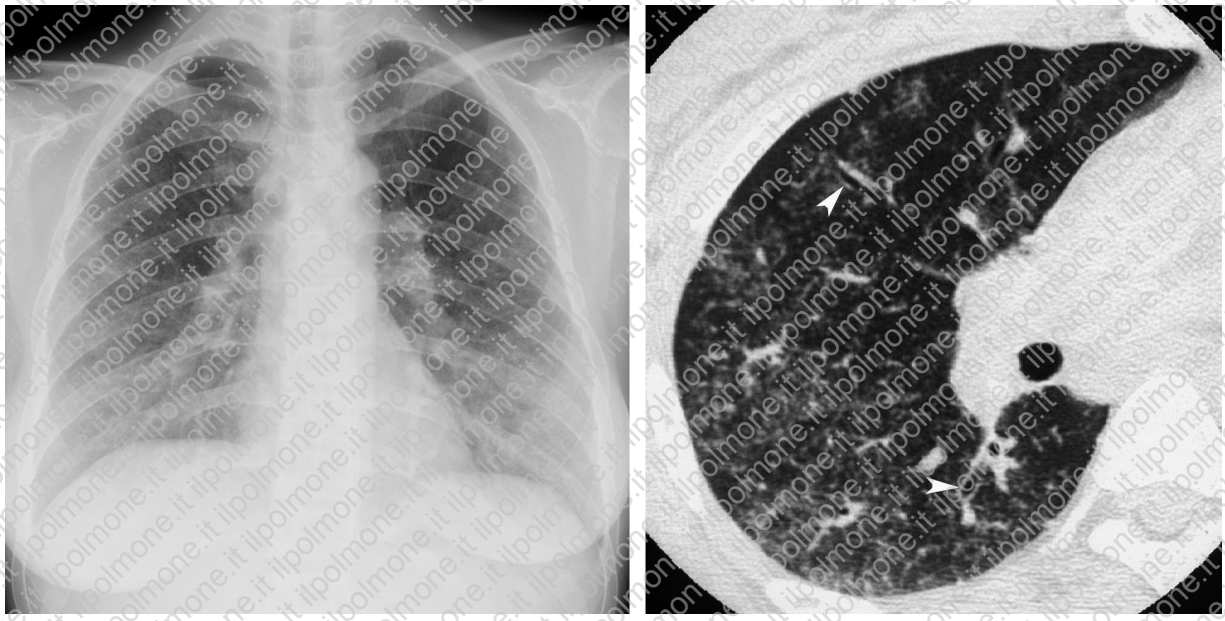

a. b.

Figure 6. Pulmonary sarcoidosis in a 31-year-old woman. **(a)** Chest radiograph shows hazy ground-glass opacity with a lower lung predominance, both of which are unusual findings. **(b)** High-resolution chest CT scan shows widespread areas of ground-glass attenuation with reticulonodular hyperattenuating areas. Mild bronchiectasis is present peripherally (arrowheads).

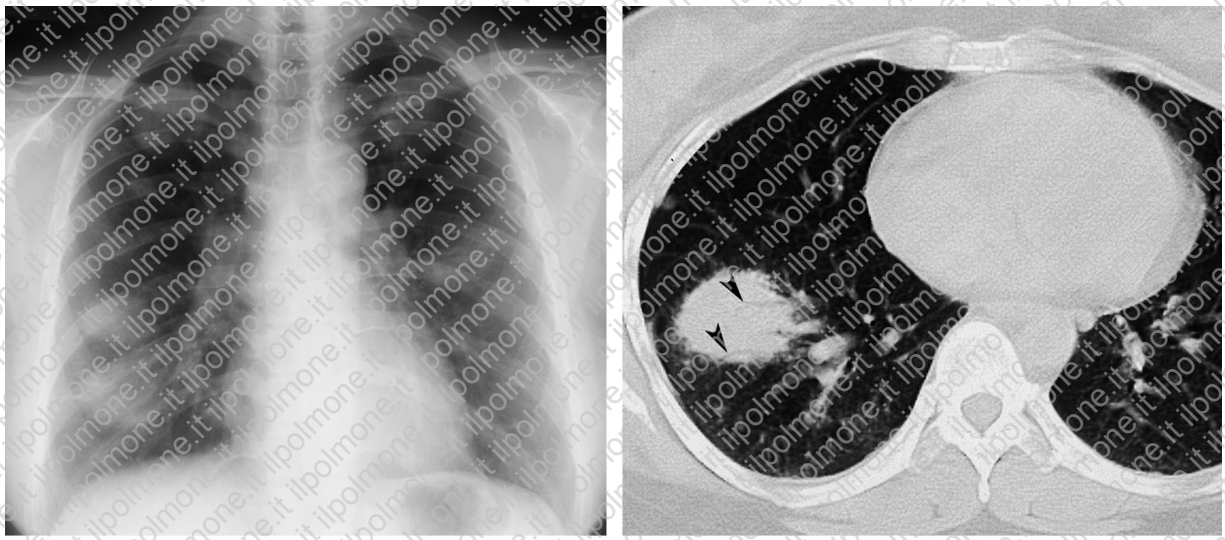

a. b.

Figure 7. Pulmonary sarcoidosis in a 26-year-old woman. **(a)** Chest radiograph demonstrates multiple lung nodules bilaterally and minimal hilar adenopathy, findings that may simulate metastatic disease. **(b)** CT scan obtained at the lower lung level demonstrates a nodular consolidation with ill-defined borders. Note the presence of an air bronchogram (arrowheads) within the nodules, a finding that is unusual for metastatic tumors.

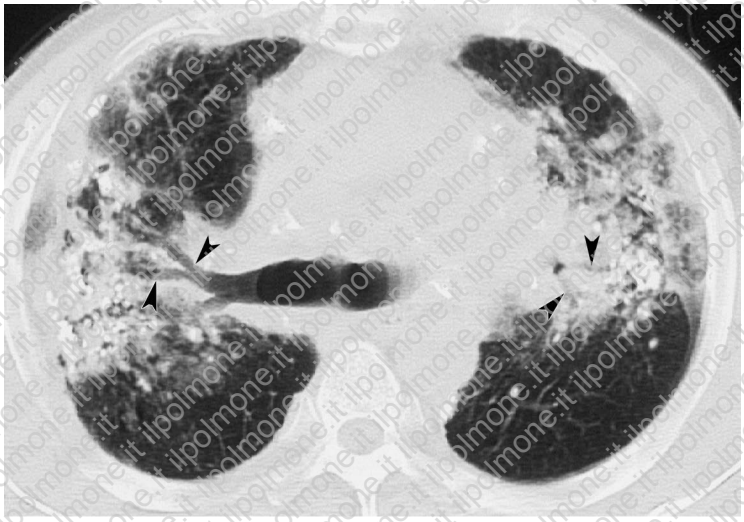

a.

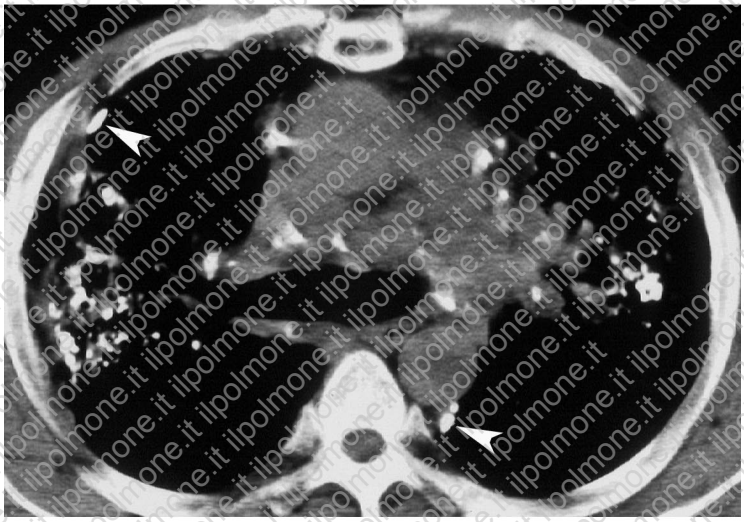

b.

Figure 8. Stage IV pulmonary sarcoidosis in a 48-year-old man. **(a)** Chest CT scan (lung window) demonstrates traction bronchiectasis (arrowheads) and fibrotic lesions with extensive calcification, findings that indicate stage IV disease. **(b)** Chest CT scan (mediastinal window) demonstrates calcification in the fibrotic lesions, mediastinal adenopathy, and irregularly thickened pleura (arrowheads).

Figure 9. Stage IV pulmonary sarcoidosis in a 60-year-old man. Chest CT scan demonstrates extensive fibrotic change and cavitary lesions with a central distribution (arrows) that distort the lung parenchyma. Irregular thickening of the pleura (arrowheads) and overinflation of the peripheral lung parenchyma are also seen.

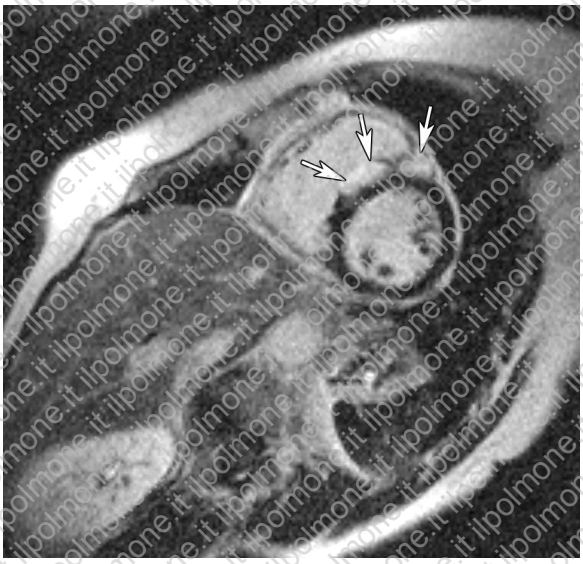

Figure 10. Cardiac sarcoidosis in a 59-year-old woman with abnormal electrocardiographic findings. Contrast-enhanced turbo fast low-angle shot inversion-recovery image (short-axis view) shows enhancement in the interventricular septum (arrows). The long-axis view was deleted.

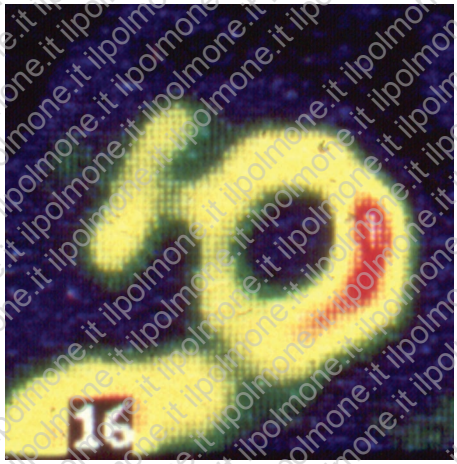

Figure 11. Cardiac sarcoidosis in a 60-year-old man who presented with complete atrioventricular blockage. Image obtained with Ga-67 citrate single photon emission computed tomography (short-axis view) shows diffuse abnormal radiotracer accumulation in the myocardium. Areas of strong uptake represent foci of increased disease activity.

End-stage (stage IV) disease may manifest as conglomerated masses with marked traction bronchiectasis (Fig 8), conditions that are probably caused by endobronchial disease (10). These processes are usually seen predominantly in the central and upper lung. Again, this distribution is typical of sarcoidosis but can also be seen in tuberculosis and silicosis. Extensive calcification may be encountered within fibrotic granulomas (6). Cavitation or cyst formation may also be seen (Fig 9). This finding is more frequently encountered in necrotizing sarcoid granulomatosis, a rare variant of sarcoidosis that is characterized by angiitis (11).

Heart

Cardiac involvement was observed in 25% of patients in an autopsy series (12). Patients can often remain asymptomatic with only abnormal electrocardiographic findings, and clinical evidence of myocardial involvement is present in only 5% of patients (2). However, involvement of the conduction pathway may result in sudden cardiac arrest. Ventricular arrhythmia, heart blockage, and congestive heart failure can also occur.

Occasionally, myocardial thinning at the site of involvement may be seen at CT. However, cardiac sarcoidosis can hardly be visualized at CT. Magnetic resonance (MR) imaging is reported to be more useful for detecting myocardial involvement in sarcoidosis. The sites of involvement manifest as areas of increased signal intensity on T2-weighted MR images or areas of enhancement on contrast-enhanced T1-weighted images (Fig 10) (13). However, the common use of a pacemaker in patients with cardiac sarcoidosis limits the usefulness of MR imaging. Gallium-67 scintigraphy is also useful for detecting cardiac sarcoidosis. Although this modality does not have a high sensitivity, it is still helpful in monitoring disease activity (Fig 11) (14).

CNS Involvement

Asymptomatic involvement of the CNS is present in up to 25% of patients at autopsy, whereas clinically recognizable involvement is seen in less than 10% of patients (15,16). Manifestations of neurosarcoidosis are variable and depend on the site and extent of involvement. The prognosis is also variable, ranging from a self-limiting process to a progressive course. Although the radiologic features of CNS sarcoidosis may simulate those of infectious or metastatic disease, mild clinical manifestations and laboratory data from cerebrospinal fluid analysis, such as increased ACE titer and CD4:CD8 ratio, may be useful in differentiating CNS sarcoidosis from other disease entities.

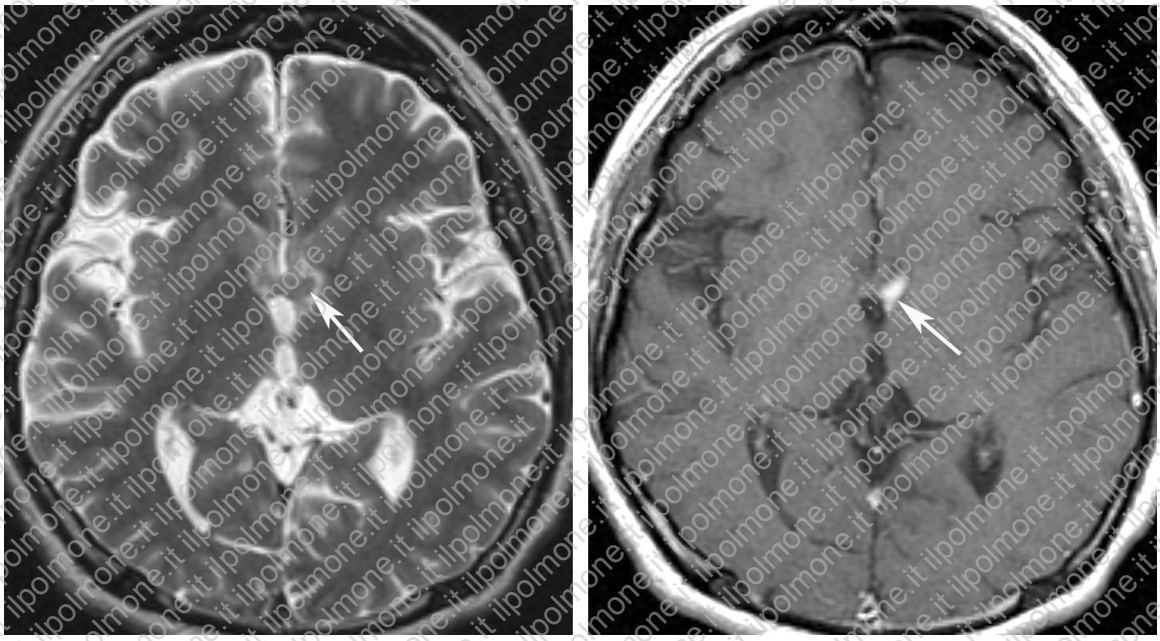

a. b.

Figure 12. Neurosarcoidosis in a 24-year-old man who presented with diabetes insipidus. **(a)** Axial T2-weighted MR image demonstrates an isointense periventricular lesion (arrow) surrounded by minimal high-signal-intensity edema. **(b)** On a contrast-enhanced T1-weighted MR image, the lesion demonstrates enhancement (arrow).

Brain

Neurosarcoidosis has a strong predilection for the base of the brain. Cranial nerve involvement, especially facial nerve palsy, is a common clinical manifestation. When bilateral facial nerve palsies develop in young adults, sarcoidosis is the most likely cause. These palsies often demonstrate rapid onset with spontaneous resolution (17). The optic nerve and chiasm are also frequently involved (18). These lesions tend to occur in the early stage of the disease, often with rapid onset, and respond to treatment or resolve spontaneously (16,17). Neuroendocrine disorders such as diabetes insipidus that arise owing to involvement of the pituitary gland and hypothalamus are relatively common, although the anterior pituitary gland is rarely involved.

MR imaging can depict a wide spectrum of parenchymal abnormalities (19). Periventricular and deep white matter lesions are commonly seen and are typically hyperintense on T2-weighted images (Fig 12) (20). Multiple or solitary parenchymal masses can be seen. These masses may have a ringlike appearance (Fig 13) and thereby mimic glioblastoma or metastases. At contrast-enhanced imaging, parenchymal lesions typically enhance while they are biologically active (Fig 12). In response to treatment, these lesions decrease in signal intensity and become unidentifiable on contrast-enhanced images (20,21).

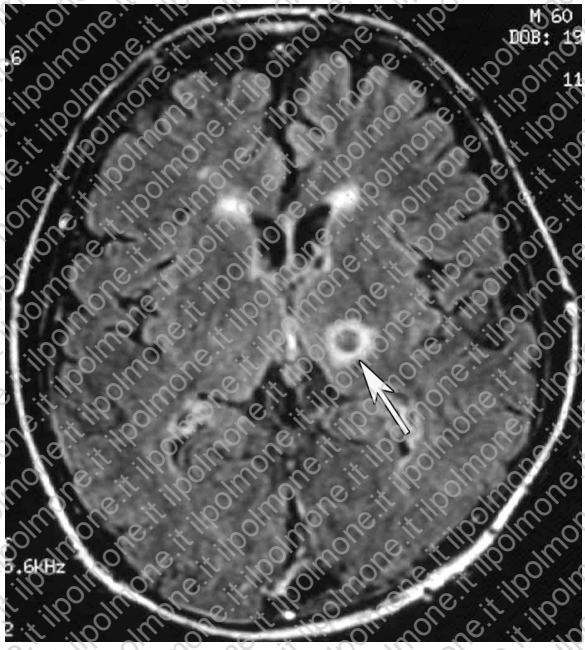

Figure 13. Neurosarcoidosis in a 60-year-old man who presented with decreased visual acuity and lower cranial nerve paresis. Axial fluid-attenuation inversion-recovery (FLAIR) MR image shows a left-sided thalamic mass with a ringlike appearance (arrow).

Chiasmatic lesions can be clearly visualized as foci of increased signal intensity on FLAIR images (Fig 14) (22). When diabetes insipidus due to involvement of the hypothalamus occurs, hyperintensity of the posterior pituitary lobe caused by intracellular neurosecretory granules is no

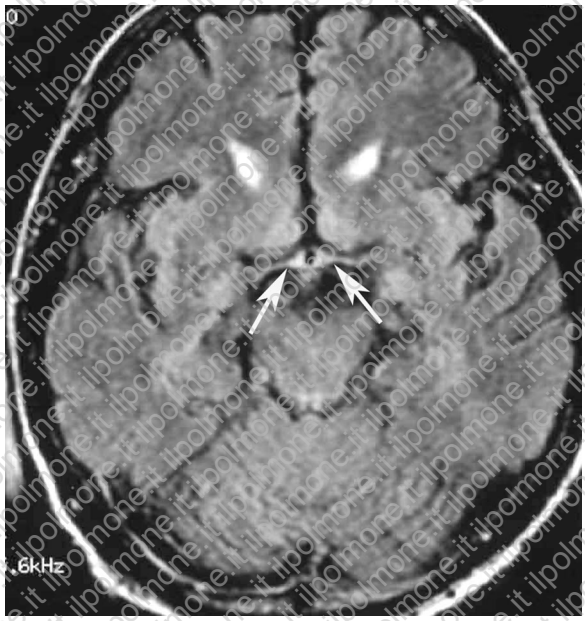

Figure 14. Neurosarcoidosis. On a FLAIR MR image obtained in the same patient as in Figure 13, the optic chiasm demonstrates increased signal intensity (arrows).

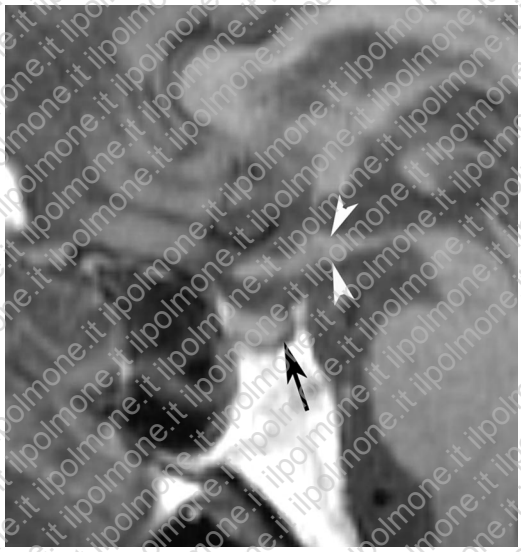

Figure 15. Neurosarcoidosis. Midsagittal T1-weighted MR image obtained in the same patient as in Figure 12 reveals an enlarged hypothalamus (arrowheads) and loss of the high signal intensity normally seen in the posterior pituitary lobe (arrow).

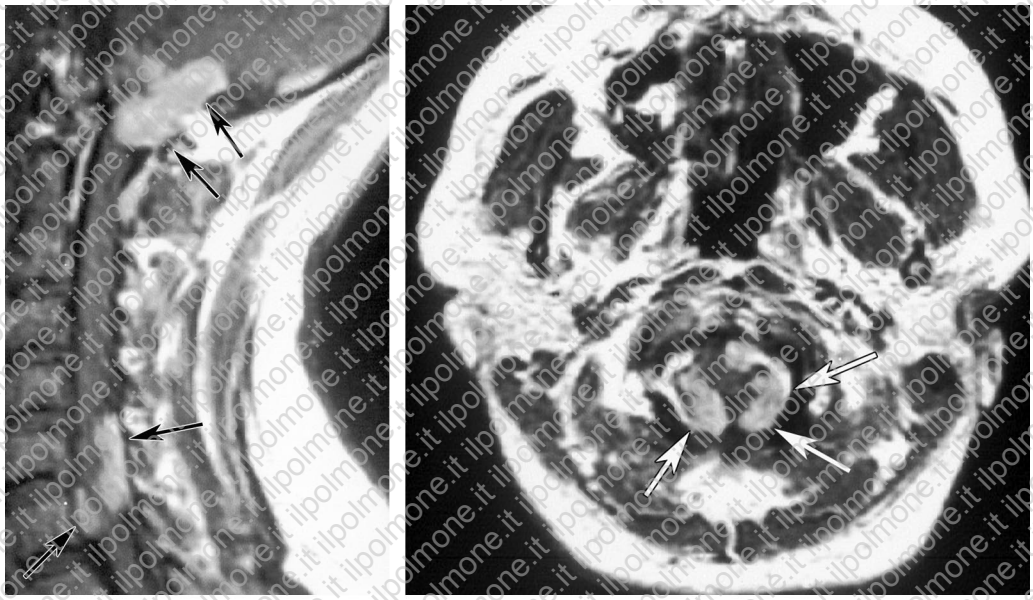

a. **b.**

Figure 16. Leptomeningeal involvement in a 23-year-old woman. Sagittal **(a)** and axial **(b)** contrast-enhanced T1-weighted MR images show diffusely enhancing leptomeningeal lesions (arrows) surrounding the upper cervical spinal cord.

longer identifiable on unenhanced T1-weighted MR images because of the depletion of granules (Fig 15) (19,23,24).

Leptomeninges

Leptomeningeal involvement, which is most commonly observed at the base of the brain, is also a frequent manifestation of CNS sarcoidosis and causes aseptic meningitis. The meningeal lesions are usually imperceptible on unenhanced MR images. Contrast-enhanced T1-weighted imaging can accurately depict diffuse enhancement in these lesions (Fig 16) (19). Less commonly, small enhancing nodules on the brain surface and in the

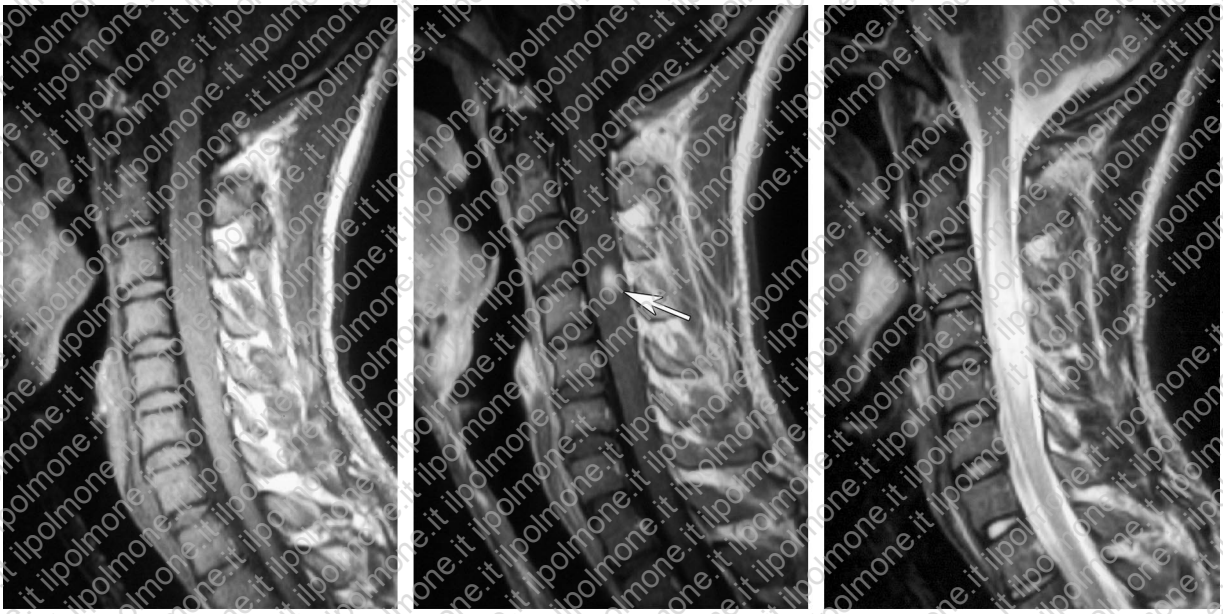

a. b. c.

Figure 18. Spinal cord involvement in a 23-year-old man who presented with mild paresis of the hands. **(a)** T1-weighted MR image shows swelling of the cervical spinal cord. **(b)** Contrast-enhanced T1-weighted MR image depicts an enhancing intramedullary lesion (arrow), a finding that represents sarcoid granuloma. **(c)** T2-weighted MR image shows associated edema with markedly increased signal intensity.

perivascular spaces may be encountered (Fig 17) (19). These radiologic appearances may occasionally mimic those of granulomatous meningitis, including tuberculosis or carcinomatous meningitis. Even relatively mild clinical findings and unremarkable CNS laboratory data may raise suspicion for sarcoidosis.

Spinal Cord

Like brain involvement, spinal cord involvement typically occurs in the early stage of the disease and responds rapidly to steroid treatment. Clinical manifestations vary depending on the site of involvement. The cervical and thoracic spinal regions are commonly involved.

T2-weighted MR images typically demonstrate an intramedullary lesion with decreased signal intensity. The spinal cord is commonly enlarged and exhibits high signal intensity due to associated edema. The focus of sarcoid granuloma demonstrates enhancement on contrast-enhanced T1-weighted images (Fig 18) (20).

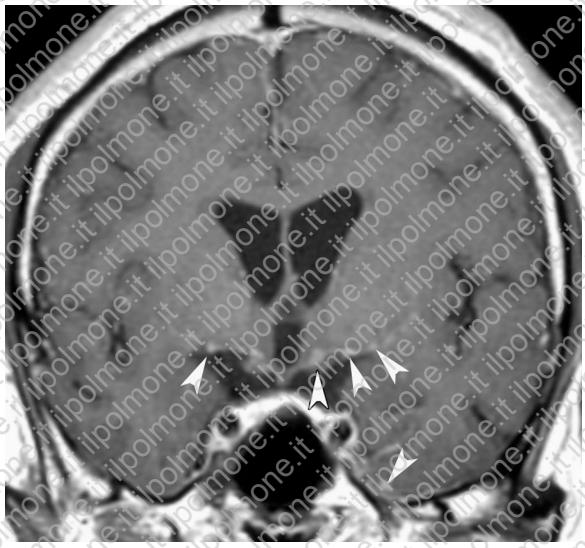

Figure 17. Leptomeningeal involvement in a 34-year-old man who presented with bilateral facial palsy. Coronal contrast-enhanced T1-weighted MR image shows enhancing miliary nodules covering the undersurface of the thalamus bilaterally, the hypothalamus, and the left temporal lobe (arrowheads).

Head and Neck Involvement

Eyes

Ocular involvement occurs in up to 80% of patients (1). Although any part of the eye or orbit can be involved, uveitis is by far the most common condition and is typically bilateral. Acute uveitis usually resolves spontaneously or responds to local corticosteroid therapy (eyedrops). Involvement of the lacrimal glands can also occur and is commonly bilateral. Contrast-enhanced CT or MR imaging typically demonstrates enlarged, enhancing lacrimal glands (Fig 19).

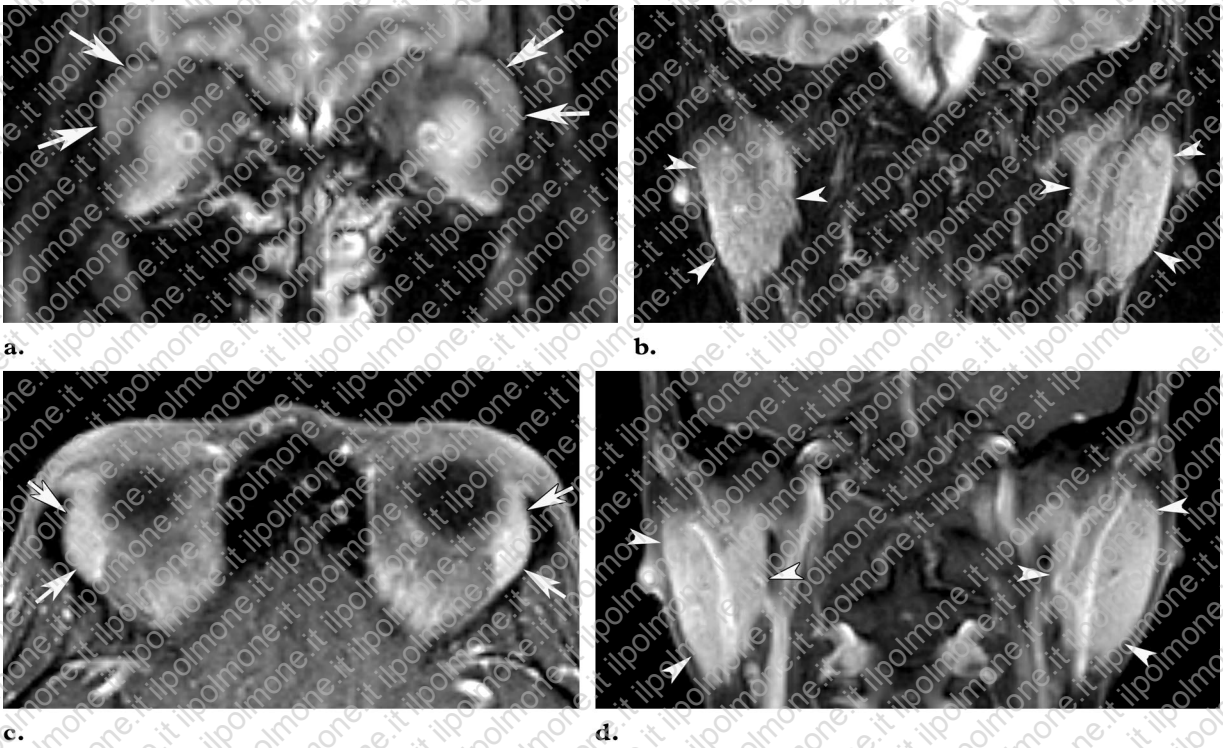

Figure 19. Ocular involvement in the same patient as in Figure 1. **(a, b)** Coronal T2-weighted MR images show symmetrically enlarged lacrimal glands (arrows in **a**) and parotid glands (arrowheads in **b**) with increased signal intensity. **(c)** Axial contrast-enhanced fat-suppressed T1-weighted MR image shows diffuse, prominent enhancement of the lacrimal glands (arrows). **(d)** Coronal contrast-enhanced fat-suppressed T1-weighted MR image also shows diffuse enhancement of the parotid glands (arrowheads). **(e)** Ga-67 scintigram demonstrates increased radiotracer accumulation in the lacrimal and parotid glands and normal accumulation in the nasopharynx, creating the mottled appearance of a giant panda ("panda sign").

Parotid Glands

Involvement of the parotid glands occurs in 6% of patients with sarcoidosis (1); it is commonly bilateral and associated with widespread disease in other organs. The combination of fever, parotid gland enlargement, facial palsy, and ocular involvement is designated as Heerfordt syndrome, which is usually a self-limiting process (25). Most patients are in the 2nd to 4th decades of life.

On MR images, affected parotid glands are typically enlarged, demonstrating increased signal intensity on T2-weighted images and enhancement on contrast-enhanced images (Fig 19). Simultaneous involvement of the parotid and lacrimal glands manifests as increased radiotracer accumulation bilaterally in these glands and normal accumulation in the nasopharynx at Ga-67 citrate scintigraphy, findings that are referred to as the panda sign (26,27). Although this sign is a classic feature of sarcoidosis, it may also be seen in other systemic diseases, including lymphoma, Sjögren syndrome, and acquired immunodeficiency syndrome. Familiarity with the clinical and radiologic features of sarcoidosis can easily help differentiate it from these other conditions.

Cervical Lymph Nodes

About one-third of patients with sarcoidosis have palpable peripheral lymphadenopathy. In the neck, nodes in the posterior triangle are more commonly affected than those in the anterior triangle. Enlarged lymph nodes are usually discrete, movable, and nontender. Recognition of cervical adenopathy at radiology is important for obtaining a biopsy specimen. However, the imaging appearances of these nodes are nonspecific.

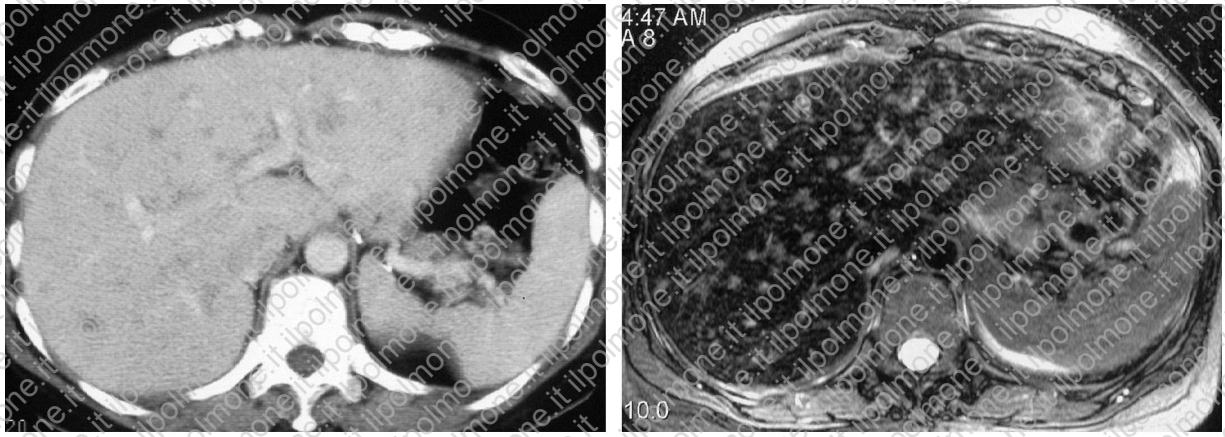

a. b.

Figure 20. Hepatic involvement in a 49-year-old woman with pulmonary sarcoidosis. **(a)** Contrast-enhanced abdominal CT scan shows multiple, irregularly shaped nodules of variable size in the liver. **(b)** T2-weighted MR image obtained after the administration of ferumoxides (Feridex; Advanced Magnetics, Cambridge, Mass) demonstrates multiple small, high-signal-intensity nodules throughout the liver.

Upper Abdominal Involvement

Liver and Spleen

Although histologic evidence of sarcoidosis involving the liver and spleen is seen in 50%–80% of autopsy specimens, dysfunction of these organs is uncommon. Asymptomatic patients who present with isolated hepatosplenic sarcoidosis do not require treatment.

At CT or MR imaging, hepatic sarcoidosis usually manifests with minimal organomegaly. In only 5%–15% of patients, coalescing granulomas become apparent as multiple hypointense or hypoattenuating nodules (Fig 20) (28). Splenic nodules are larger and more common than hepatic lesions (Figs 21, 22) (28). Affected patients frequently have abdominal or systemic symptoms and elevated ACE levels, although 25% of patients have normal findings at chest radiography.

Multiple nodules in hepatic sarcoidosis are easily mistaken for more common diseases, including metastases and lymphoma. In these conditions, screening for malignancy may be required. Simultaneous involvement of the spleen favors a diagnosis of sarcoidosis and lymphoma. Investigation of laboratory data, including tumor markers or soluble interleukin-2 receptors, can also be useful in differentiating sarcoidosis from malignant lymphoma or other malignancies. When there is no other clinical evidence of sarcoidosis, liver biopsy may be considered. Rarely, diffuse granulomatous involvement along the periportal tract can cause subsequent fibrosis with a cirrhotic appearance (Fig 22) (29).

Figure 21. Splenic involvement in the same patient as in Figure 5. Contrast-enhanced abdominal CT scan demonstrates multiple small, hypoattenuating nodules scattered diffusely throughout the spleen.

Gastrointestinal Tract

Gastrointestinal tract involvement has a prevalence of less than 1% and is usually associated with pulmonary disease. The stomach is the most common site of involvement, although sarcoidosis has been reported in every part of the gastrointestinal tract (30). Gastric sarcoidosis has a predilection for the antrum. Radiologic appearances range from ulceration resembling peptic ulcer disease, to mucosal thickening mimicking Menetrier disease, to linitis plastica resembling scirrhous carcinoma. Diagnosis of gastric involvement requires endoscopic biopsy. Because most patients with gastric sarcoidosis remain asymptomatic, clinical suspicion for gastrointestinal involvement may not be forthcoming.

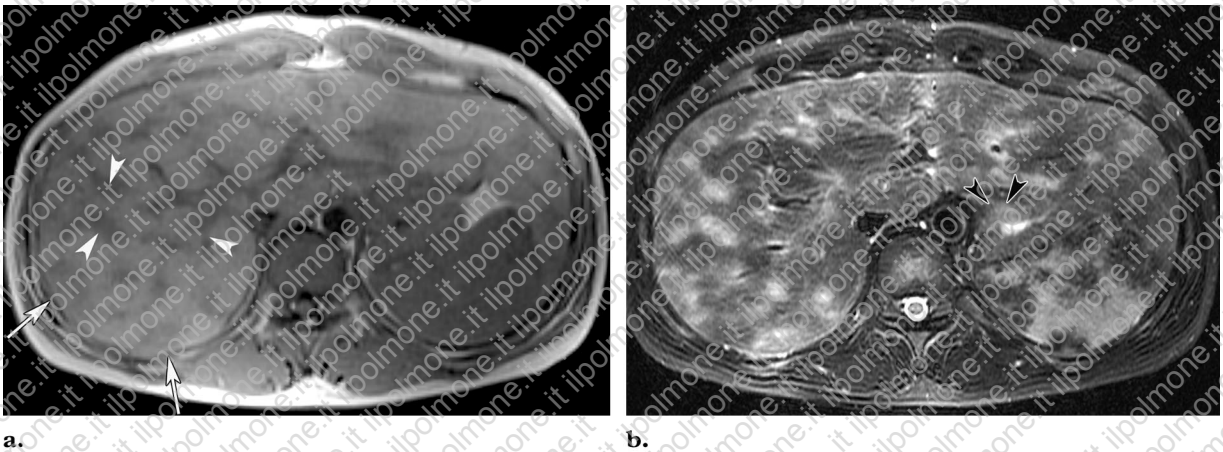

Figure 22. Splenic involvement in the same patient as in Figure 6. **(a)** Unenhanced gradient-echo T1-weighted MR image of the upper abdomen demonstrates irregularly shaped, low-signal-intensity nodules peripherally in the liver (arrows) and widening of the periportal tract (arrowheads). **(b)** On a T2-weighted MR image of the upper abdomen, the peripheral liver nodules demonstrate increased signal intensity. Multiple hypointense nodules in the spleen create a heterogeneous appearance. The area of focal hyperintensity (arrowheads) represents gastric mucosal involvement. **(c)** Ferumoxides-enhanced gradient-echo T2*-weighted MR image shows multiple hyperintense nodules scattered throughout the periphery of the liver (arrows) and a hyperintense, widened periportal tract.

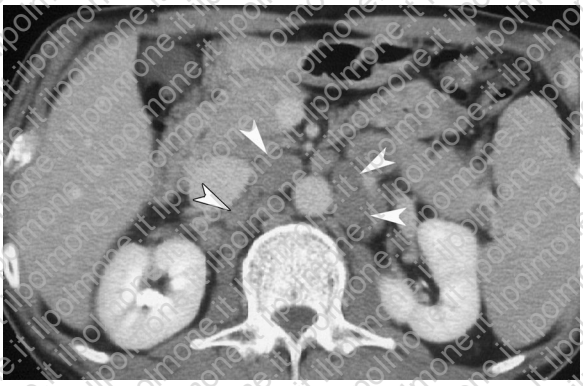

Figure 23. Lymphadenopathy in the paraaortic region in the same patient as in Figure 9. Contrast-enhanced abdominal CT scan shows multiple paraaortic areas of adenopathy (arrowheads) that mimic lymphoma or metastases.

Abdominal Lymph Nodes

Massive lymphadenopathy in the paraaortic region is rare but may be encountered in patients with systemic sarcoidosis (Fig 23). Imaging findings in these nodes are usually nonspecific, and differentiation from metastatic carcinoma or malignant lymphoma may be difficult. At histologic analysis, abdominal lymph node involvement needs to be differentiated from tumor-related sarcoid reaction. The former is characterized by noncaseating granulomas in regional lymph nodes (eg, gastric cancer) (31).

Genitourinary Involvement

In autopsy series, sarcoidosis of the genitourinary tract is seen in 5% of patients. In the majority of these cases, involvement is confined to the kidneys. To a lesser extent, involvement of the epididymis and testis can also be seen. In most cases, the diagnosis of sarcoidosis is made before genitourinary involvement occurs.

Kidneys

Renal manifestations of sarcoidosis are commonly related to nephrocalcinosis, which results from hypercalcemia. On occasion, the granulomatous process can directly involve the kidney, producing interstitial nephritis and glomerulonephritis.

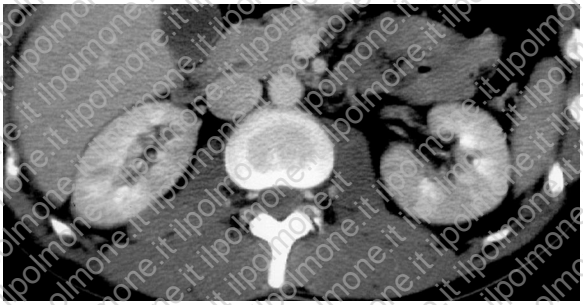

Figure 24. Renal involvement in the same patient as in Figures 1 and 19. Contrast-enhanced CT scan shows striated nephrograms in both kidneys. Renal function was within the normal range.

Detection of renal involvement depends on radiologic studies because renal function usually remains within the normal range. Contrast-enhanced CT may show striated nephrograms in cases of interstitial nephritis (Fig 24). In rare instances, renal sarcoidosis manifests as multiple low-attenuation tumorlike nodules (Fig 25) that can mimic lymphoma or metastatic tumors (32,33).

Scrotum

In intrascrotal sarcoidosis, epididymitis is the most common form of involvement and is bilateral in one-third of cases (34). Epididymitis is commonly asymptomatic, but patients may present with pain or a scrotal mass. Testicular involvement can be associated with epididymitis and is typically bilateral and multiple. Isolated involvement of the testis is very rare. A diagnosis of sarcoidosis should be strongly considered in cases of multiple masses that simultaneously affect the epididymis and testis. Ultrasonography (US) and MR imaging display bilaterally enlarged epididymides (Fig 26). Testicular lesions appear as multiple nodules with decreased echogenicity at US. At MR imaging, these lesions exhibit low signal intensity on T2-weighted images and enhancement on contrast-enhanced T1-weighted images (Fig 26) (35).

Figure 25. Renal sarcoidosis in a 71-year-old man who presented with swelling of the distal right thigh. Contrast-enhanced CT scan demonstrates multiple hypoattenuating nodules in both kidneys (arrows). The right kidney also contains a large renal cyst.

Musculoskeletal Involvement

Musculoskeletal involvement in sarcoidosis usually occurs in patients with generalized disease. Although involvement of the joints is common, the presence of muscle and bone lesions is unusual and is believed to indicate a chronic and prolonged clinical course.

Joints

Musculoskeletal involvement often manifests as inflammatory arthralgia (up to 40% of cases) (1). The joints most commonly affected are the knees, ankles, elbows, and wrists. However, radiologically identifiable abnormalities are rare. The combination of erythema nodosum, periarticular ankle inflammation, and mediastinal lymphadenopathy is designated as Löfgren syndrome, which usually has a self-limiting course with spontaneous resolution (36).

Muscles

When sarcoidosis involves the skeletal muscles, myopathic or nodular type involvement can occur (37). The latter is clinically problematic because it may be confused with a soft-tissue tumor. Nodular type involvement has a characteristic appearance at MR imaging that may allow accurate diagnosis. The sarcoid nodules typically consist of central areas of fibrosis that demonstrate

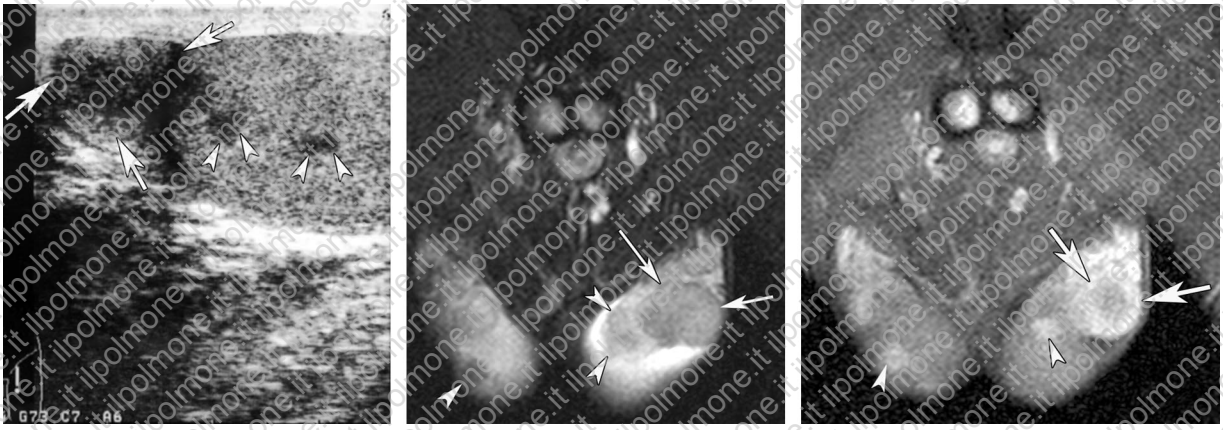

a. b. c.

Figure 26. Intrascrotal sarcoidosis in a 16-year-old boy who presented with epididymal pain and swelling. **(a)** US image of the scrotum (longitudinal view) demonstrates a markedly enlarged left epididymis (arrows) and multiple hypoechoic nodules in the left testis (arrowheads). **(b, c)** T2-weighted **(b)** and contrast-enhanced **(c)** MR images show an enlarged left epididymis (arrows) and multiple nodules in both testes (arrowheads). The nodules are hypointense on the T2-weighted image and demonstrate enhancement on the contrast-enhanced image.

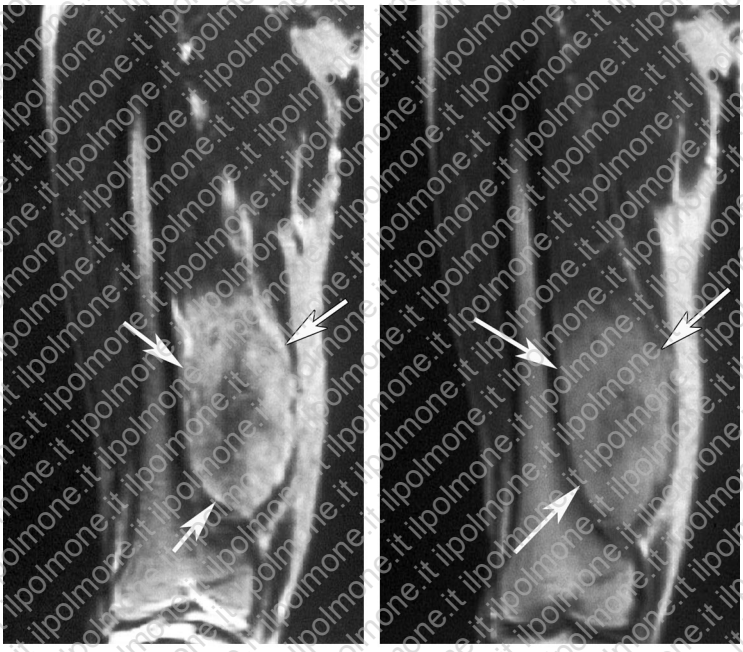

a. b.

Figure 27. Nodular type muscle involvement in the same patient as in Figure 25. T2-weighted **(a)** and contrast-enhanced **(b)** MR images demonstrate a nodular type muscle lesion (arrows). The lesion has a central area of decreased signal intensity (as it did with all sequences). The periphery of the lesion demonstrates increased signal intensity on the T2-weighted image and prominent enhancement on the contrast-enhanced image.

low signal intensity with all sequences and peripheral areas of granulomas that exhibit bright signal intensity on T2-weighted images and enhancement on contrast-enhanced images (Fig 27) (37). In myopathic type involvement, MR imaging findings are nonspecific. The involved muscle has increased signal intensity on T2-weighted images.

Bones

Skeletal involvement is seen in approximately 5%–10% of patients with sarcoidosis. The phalanges in the hands and feet are most frequently affected. These lesions are often multiple, and

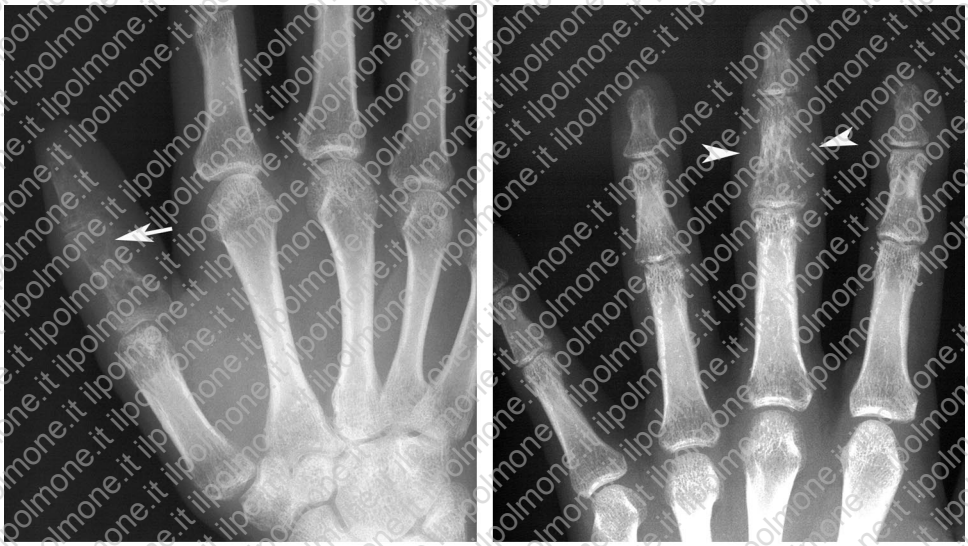

a. b.

Figure 28. Bone sarcoidosis in a 28-year-old man who presented with left thumb pain. **(a)** Close-up view from a radiograph of the left hand shows a pathologic fracture caused by an extensive osteolytic lesion in the thumb (arrow). **(b)** Close-up view from a radiograph of the right hand reveals a radiolucent lesion in the middle phalanx of the third finger. The lesion has a lacelike appearance and is accompanied by a soft-tissue mass (arrowheads). This combination of findings is virtually diagnostic for bone sarcoidosis.

nuclear scintigraphic findings are usually positive even before the lesions manifest at radiography.

Radiologic features may include cystlike radiolucent areas, a lacelike honeycomb appearance, or extensive bone erosion with pathologic fractures (Fig 28) (38). The articular spaces are usually intact, unless extensive neuropathic lesions develop. A subcutaneous soft-tissue mass or tenosynovitis may also be present. The combination of these radiologic features is virtually diagnostic.

Involvement of other skeletal structures may also be encountered but is hard to diagnose correctly. Even pathologic analysis of a biopsy specimen may lead to misdiagnosis of a lesion as tuberculosis. In the long bones, lesions may manifest as well-defined defects or permeating destruction. In the vertebrae, sarcoidosis can cause osteolytic lesions, whereas the disk spaces are usually preserved (Fig 29). Widespread sclerosis may also be seen in the vertebrae (39).

Cutaneous Involvement

Although skin lesions are not the subject of radiologic studies, familiarity with cutaneous sarcoidosis will be helpful in establishing the diagnosis. Cutaneous involvement occurs in approximately 25% of patients and encompasses a wide variety of dermatologic diseases (40). However, two types of cutaneous lesions are especially important and known classically: erythema nodosum and lupus pernio. Erythema nodosum, a hallmark of acute sarcoidosis, manifests as tender red bumps or nodules on the anterior aspects of the legs and is frequently associated with arthralgia (Löfgren syndrome). Lupus pernio manifests as indurated plaques with discoloration around the face. This condition is seen in chronic sarcoidosis and is frequently associated with pulmonary fibrosis.

Conclusions

Sarcoidosis has a wide variety of clinical and radiologic manifestations. Because the disease frequently involves multiple organs, familiarity with the clinical and radiologic features of sarcoidosis in various anatomic locations plays a crucial role in diagnosis and management.

Acknowledgments: We wish to express our sincere thanks to Yukio Miki, MD, Kyo Itoh, MD, Eiji Tadamura, MD, and Hideaki Yoshimura, MD for recruiting cases. We also thank Toshitaka Fujiwara, MD, Takayuki Yamamoto, and Soji Nishio for their cooperation.

References

1. Statement on sarcoidosis: Joint Statement of the American Thoracic Society (ATS), the European Respiratory Society (ERS) and the World Associa-

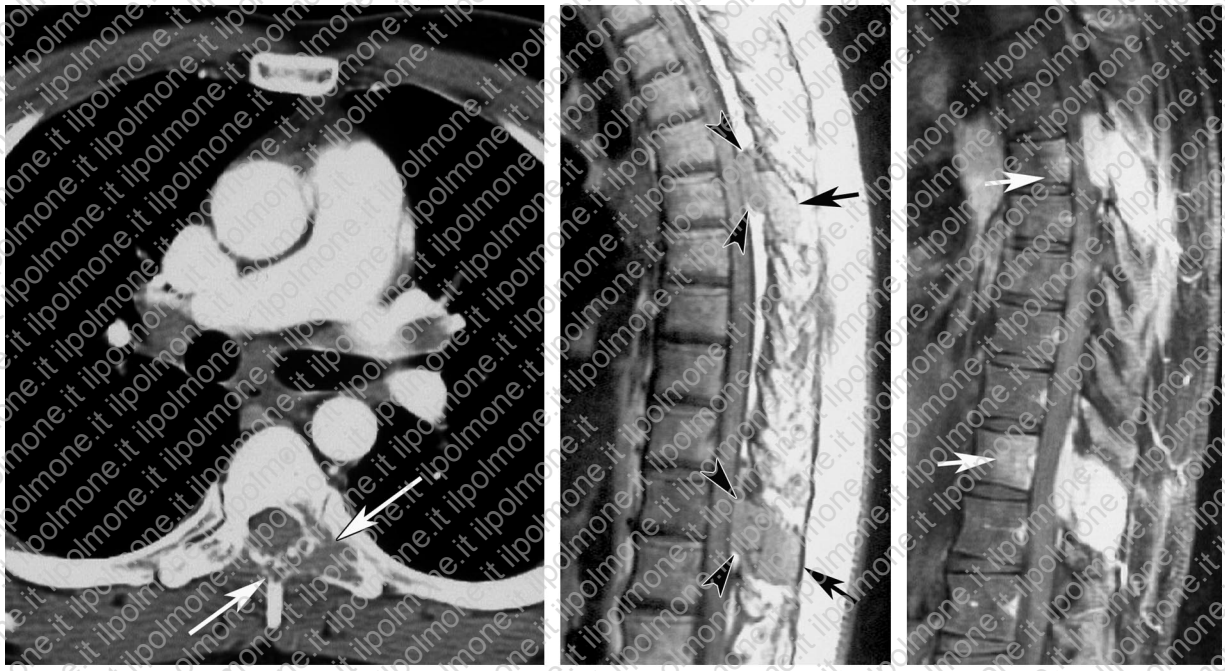

a. b. c.

Figure 29. Bone sarcoidosis in the same patient as in Figure 2. **(a)** Contrast-enhanced CT scan demonstrates an osteolytic lesion in the posterior portion of the sixth thoracic vertebra (arrows). Bilateral hilar lymphadenopathy is also present. **(b)** Sagittal unenhanced T1-weighted MR image demonstrates multiple lesions in the posterior portion of the thoracic vertebrae. The lesions extend into the epidural spaces (arrowheads) and adjacent soft tissue (arrows). **(c)** On a contrast-enhanced fat-suppressed T1-weighted MR image, the lesions display diffuse enhancement. The presence of enhancement in the vertebral bodies (arrows) suggests disease involvement.

tion of Sarcoidosis and Other Granulomatous Disorders (WASOG) adopted by the ATS Board of Directors and by the ERS Executive Committee, February 1999. Am J Respir Crit Care Med 1999; 160:736–755.

2. Iwai K, Sekiguti M, Hosoda Y, et al. Racial difference in cardiac sarcoidosis incidence observed at autopsy. Sarcoidosis 1994; 11:26–31.
3. Gideon NM, Mannino DM. Sarcoidosis mortality in the United States 1979–1991: an analysis of multiple-cause mortality data. Am J Med 1996; 100:423–427.
4. Miller BH, Rosado-de-Christenson ML, McAdams HP, Fishback NF. Thoracic sarcoidosis: radiologic-pathologic correlation. RadioGraphics 1995; 15:421–437.
5. Conant EF, Glickstein MF, Mahar P, Miller WT. Pulmonary sarcoidosis in the older patient: conventional radiographic features. Radiology 1988; 169:315–319.
6. Rockoff SD, Rohatgi PK. Unusual manifestations of thoracic sarcoidosis. AJR Am J Roentgenol 1985; 144:513–528.
7. Kitaichi M. Pathology of pulmonary sarcoidosis. Clin Dermatol 1986; 4:108–115.
8. Nishimura K, Itoh H, Kitaichi M, Nagai S, Izumi T. Pulmonary sarcoidosis: correlation of CT and histopathologic findings. Radiology 1993; 189: 105–109.
9. Muller NL, Kullnig P, Miller RR. The CT findings of pulmonary sarcoidosis: analysis of 25 patients. AJR Am J Roentgenol 1989; 152:1179–1182.
10. Brauner MW, Grenier P, Mompoint D, Lenoir S, de Cremoux H. Pulmonary sarcoidosis: evaluation with high-resolution CT. Radiology 1989; 172: 467–471.
11. Niimi H, Hartman TE, Muller NL. Necrotizing sarcoid granulomatosis: computed tomography and pathologic findings. J Comput Assist Tomogr 1995; 19:920–923.
12. Ratner SJ, Fenoglio JJ, Jr, Ursell PC. Utility of endomyocardial biopsy in the diagnosis of cardiac sarcoidosis. Chest 1986; 90:528–533.
13. Vignaux O, Dhote R, Duboc D, et al. Clinical significance of myocardial magnetic resonance abnormalities in patients with sarcoidosis: a 1-year follow-up study. Chest 2002; 122:1895–1901.
14. Mana J. Magnetic resonance imaging and nuclear imaging in sarcoidosis. Curr Opin Pulm Med 2002; 8:457–463.
15. Manz HJ. Pathobiology of neurosarcoidosis and clinicopathologic correlation. Can J Neurol Sci 1983; 10:50–55.
16. Chapelon C, Ziza JM, Piette JC, et al. Neurosarcoidosis: signs, course and treatment in 35 confirmed cases. Medicine (Baltimore) 1990; 69:261–276.

17. Sharma OP. Neurosarcoidosis: a personal perspective based on the study of 37 patients. Chest 1997; 112:220–228.
18. Zajicek JP, Scolding NJ, Foster O, et al. Central nervous system sarcoidosis: diagnosis and management. QJM 1999; 92:103–117.
19. Sherman JL, Stern BJ. Sarcoidosis of the CNS: comparison of unenhanced and enhanced MR images. AJNR Am J Neuroradiol 1990; 11:915–923.
20. Lexa FJ, Grossman RI. MR of sarcoidosis in the head and spine: spectrum of manifestations and radiographic response to steroid therapy. AJNR Am J Neuroradiol 1994; 15:973–982.
21. Zouaoui A, Maillard JC, Dormont D, Chiras J, Marsault C. MRI in neurosarcoidosis. J Neuroradiol 1992; 19:271–284.
22. Bode MK, Tikkakoski T, Tuisku S, Kronqvist E, Tuominen H. Isolated neurosarcoidosis: MR findings and pathologic correlation. Acta Radiol 2001; 42:563–567.
23. Colombo N, Berry I, Kucharczyk J, et al. Posterior pituitary gland: appearance on MR images in normal and pathologic states. Radiology 1987; 165: 481–485.
24. Fujisawa I, Nishimura K, Asato R, et al. Posterior lobe of the pituitary in diabetes insipidus: MR findings. J Comput Assist Tomogr 1987; 11:221–225.
25. James DG, Sharma OP. Parotid gland sarcoidosis. Sarcoidosis Vasc Diffuse Lung Dis 2000; 17:27–32.
26. Kurdziel KA. The panda sign. Radiology 2000; 215:884–885.
27. Sulavik SB, Spencer RP, Castriotta RJ. Panda sign: avid and symmetrical radiogallium accumulation in the lacrimal and parotid glands. Semin Nucl Med 1991; 21:339–340.
28. Warshauer DM, Molina PL, Hamman SM, et al. Nodular sarcoidosis of the liver and spleen: analysis of 32 cases. Radiology 1995; 195:757–762.
29. Mergo PJ, Ros PR, Buetow PC, Buck JL. Diffuse disease of the liver: radiologic-pathologic correlation. RadioGraphics 1994; 14:1291–1307.
30. Farman J, Ramirez G, Rybak B, Lebwohl O, Semrad C, Rotterdam H. Gastric sarcoidosis. Abdom Imaging 1997; 22:248–252.
31. Kojima M, Nakamura S, Fujisaki M, et al. Sarcoid-like reaction in the regional lymph nodes and spleen in gastric carcinoma: a clinicopathologic study of five cases. Gen Diagn Pathol 1997; 142: 347–352.
32. Sato A. Renal dysfunction in patients with sarcoidosis. Intern Med 1996; 35:523–524.
33. Hughes JJ, Wilder WM. Computed tomography of renal sarcoidosis. J Comput Assist Tomogr 1988; 12:1057–1058.
34. Ulbright TM, Amin MB, Young RH. Miscellaneous primary tumors of the testis, adnexa, and spermatic cord. In: Rosai JS, ed. Atlas of tumor pathology: tumor of the testis, adnexa, spermatic cord, and scrotum, fasc 25, ser 3. Washington, DC: Armed Forces Institute of Pathology, 1999; 235–366.
35. Woodward PJ, Sohaey R, O'Donoghue MJ, Green DE. From the archives of the AFIP: tumors and tumorlike lesions of the testis—radiologic-pathologic correlation. RadioGraphics 2002; 22:189–216.
36. Mana J, Gomez-Vaquero C, Montero A, et al. Lofgren's syndrome revisited: a study of 186 patients. Am J Med 1999; 107:240–245.
37. Otake S, Ishigaki T. Muscular sarcoidosis. Semin Musculoskelet Radiol 2001; 5:167–170.
38. Neville E, Carstairs LS, James DG. Sarcoidosis of bone. Q J Med 1977; 46:215–227.
39. Poyanli A, Poyanli O, Sencer S, Akan K, Sayrak H, Acunas B. Vertebral sarcoidosis: imaging findings. Eur Radiol 2000; 10:92–94.
40. Sharma OP. Cutaneous sarcoidosis: clinical features and management. Chest 1972; 61:320–325.

This article meets the criteria for 1.0 credit hour in category 1 of the AMA Physician's Recognition Award. To obtain credit, see accompanying test at http://www.rsna.org/education/rg_cme.html.